

InSb based Quantum Dot Nanostructures for Mid-Infrared Photonic Devices

P. J. Carrington^{*a}, E. Repiso^b, Q. Lu^b, H. Fujita^c, A.R.J. Marshall^b, Q. Zhuang^b and A. Krier^b

(a) Department of Engineering, Lancaster University, Lancaster, LA1 4YW, UK

(b) Physics Department, Lancaster University, Lancaster LA1 4YB, UK

(c) Asahi Kasei Corporation, 2-1 Samejima, Fuji-city, Shizuoka 416-8501, Japan

ABSTRACT

Novel InSb quantum dot (QD) nanostructures grown by molecular beam epitaxy (MBE) are investigated in order to improve the performance of light sources and detectors for the technologically important mid-infrared (2-5 μm) spectral range. Unlike the InAs/GaAs system which has a similar lattice mismatch, the growth of InSb/InAs QDs by MBE is a challenging task due to Sb segregation and surfactant effects. These problems can be overcome by using an Sb-As exchange growth technique to realize uniform, dense arrays (dot density $\sim 10^{12} \text{ cm}^{-2}$) of extremely small (mean diameter $\sim 2.5 \text{ nm}$) InSb submonolayer QDs in InAs. Light emitting diodes (LEDs) containing ten layers of InSb QDs exhibit bright electroluminescence peaking at 3.8 μm at room temperature. These devices show superior temperature quenching compared with bulk and quantum well (QW) LEDs due to a reduction in Auger recombination. We also report the growth of InSb QDs in InAs/AlAsSb 'W' QWs grown on GaSb substrates which are designed to increase the electron-hole (e-h) wavefunction overlap to $\sim 75\%$. These samples exhibit very good structural quality and photoluminescence peaking near 3.0 μm at low temperatures.

Keywords: Mid-infrared, Quantum Dots, InSb, Molecular beam epitaxy, Photoluminescence

1. Introduction

There is continuous worldwide interest in the development of light sources and detectors for the mid-infrared (2-5 μm) spectral range driven by the extensive range of potential applications, including environmental gas monitoring, non-invasive medical diagnosis, tunable infrared spectroscopy and free space optical communications. A number of different semiconductor materials and devices are currently being investigated including bulk AlInSb alloys¹, InGaAsSb/AlGaInAsSb quantum wells (QWs)² and InAs/GaSb superlattices³. Using quantum dots (QDs) in the active region of mid-infrared devices could offer significant advantages. The delta-like density of states inherent to the QDs leads to higher radiative transition rates, narrower spectral linewidth and the possibility to minimize Auger recombination. The most promising QD system for emission beyond 3 μm is InSb/InAs QDs which has a type II broken gap alignment (i.e., the valence band of InSb is higher than the conduction band of InAs), and radiative recombination is spatially indirect between electrons localized in the InAs matrix and holes in the confined states of the InSb QDs as shown in figure 1. Unlike the InAs/GaAs system which has a similar lattice mismatch, InSb QDs are difficult to grow by MBE due to Sb segregation and surfactant effects⁴. To overcome these problems, we developed an alternative strategy based on InSb submonolayers to grow high density (dot density $\sim 10^{12} \text{ cm}^{-2}$) coherently strained InSb QDs⁵. Light emitting diodes (LEDs) containing 10 layers of InSb/InAs QDs in the active region exhibited bright room temperature mid-infrared electroluminescence (EL). In this paper, we elucidate important new information about the temperature and current dependences of type II confined transitions in the InSb QD LEDs which exhibit superior temperature quenching due to the reduction in Auger recombination. We also report the growth of new structures based on InSb quantum dots in InAs/AlAsSb quantum wells (DWELL) grown on GaSb substrates. This enables the electron-hole wavefunction overlap

* p.carrington@lancaster.ac.uk

to be increased to ~75% by confining the electrons inside the InAs QWs, and offers the possibility to grow on technologically mature GaSb substrates.

2. MBE Growth and Device Fabrication

InSb/InAs QD LEDs (figure 1a) were grown on n-InAs (001) substrates using a VG-V80H MBE reactor. Thermal effusion K-cells were used to supply the In, Ga and Al fluxes, and two (Veeco) valved cracker cells were used to provide Sb₂ and As₂. *In-situ* reflection high energy electron diffraction (RHEED) was employed to control surface reconstruction. The substrate temperature was measured using an infrared pyrometer calibrated using surface reconstruction transitions under a fixed As flux. A 0.5 μm n-type (Te) InAs layer was first grown at 480°C, followed by 0.5 μm of nominally undoped InAs. Then ten InSb QD sheets of 0.7 monolayer thickness were grown at 430°C with 17 nm InAs barriers. The QDs were formed by exposing the InAs growth surface to Sb₂ for 20 seconds, creating a very efficient Sb-to-As anion exchange reaction followed by a short InSb deposition using migration enhanced epitaxy (MEE). Finally, an undoped 30 nm Al_{0.9}Ga_{0.1}As_{0.15}Sb_{0.85} electron blocking barrier was grown 100 nm above the active region and a 0.5 μm InAs p-type (Be) layer grown at 480°C. High structural quality was confirmed by x-ray diffraction which showed pronounced high order satellite peaks and Pendellosung fringes (figure 1c). Transmission Electron Microscopy studies revealed excellent structural quality with no stacking faults and low defect density (<10⁶ cm⁻²). Figure 1b shows a bright-field scanning transmission electron microscopy (STEM) image of a single InSb sub-monolayer QD. The size distribution of the QDs was found to be 2-3 nm high, 3-5 nm long and density ~10¹² cm⁻².

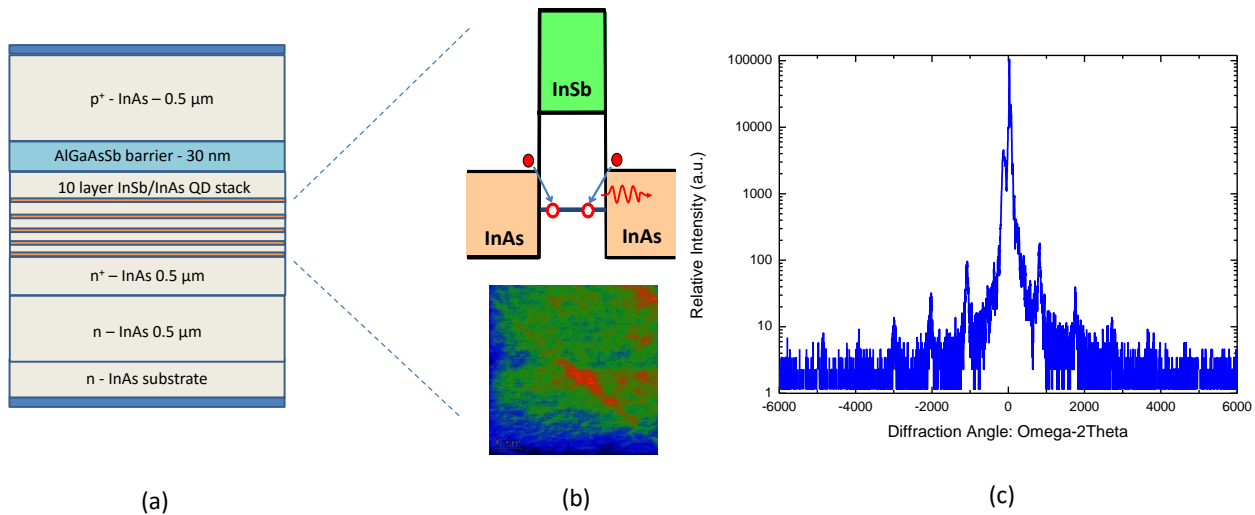


Figure 1: (a) Schematic of the InSb/InAs QD LED (b) InSb/InAs QD band lineup and Bright-field (BF) STEM image of a single InSb QD (c) High Resolution x-ray diffraction spectra obtained from the InSb/InAs QD LED.

The structure was then processed into 750 μm diameter, mesa-etched LEDs using standard photolithography and processing techniques. The LEDs were mounted epi-side up onto To-49 headers. These were placed in a continuous-flow liquid helium cryostat and EL was measured in the range 4-300K using a Bentham 0.3 m monochromator and a 77 K InSb photodiode detector. The current-voltage (I-V) curves measured from one of the LEDs are shown in figure 2. The series resistance was calculated to be ~0.9 Ω and the leakage current was around 2 mA at 0.5 V reverse bias.

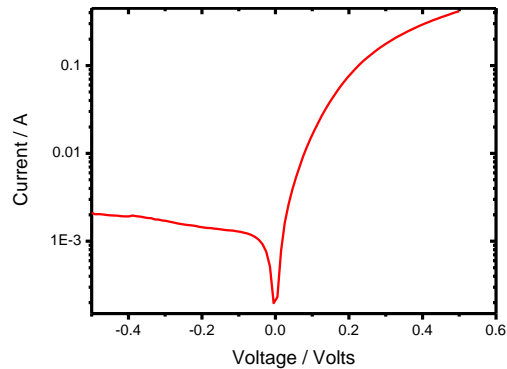


Figure 2: I-V curves measured from the InSb/InAs LEDs.

3. InSb/InAs QD Electroluminescence

The 4K EL emission spectra from one of the LEDs is shown in figure 3(a) using 20-200 mA injection current and a duty cycle of 50% at 1 kHz. The spectra can be fitted by four Gaussian functions as shown in figure 3b for 100 mA. Peaks from InAs can be observed at 0.411 and 0.435 eV originating from bound exciton and band-to-band transitions respectively. Peaks around 0.380 and 0.346 eV correspond to recombination of electrons in the InAs layers with confined heavy hole states in the InSb QDs. A blueshift of the QD emission peaks is observed as the current is increased. Such blueshifts in type II QD systems are attributed to the combination of occupation of excited states and capacitive coulomb charging, rather than to the band bending at the type II interface⁶. At 4 K, the peaks from InAs are much stronger than the InSb QD peaks which is opposite to that observed in photoluminescence (PL)⁷. This is due to the increased carrier concentration in EL ($\sim 5 \times 10^{17} \text{cm}^{-3}$ in EL compared to 10^{14}cm^{-3} in PL) and the use of the AlGaAsSb barrier which prevents injected electrons diffusing away from the active region, causing a decrease in the QD emission relative to the InAs emission due to band filling in the QD array.

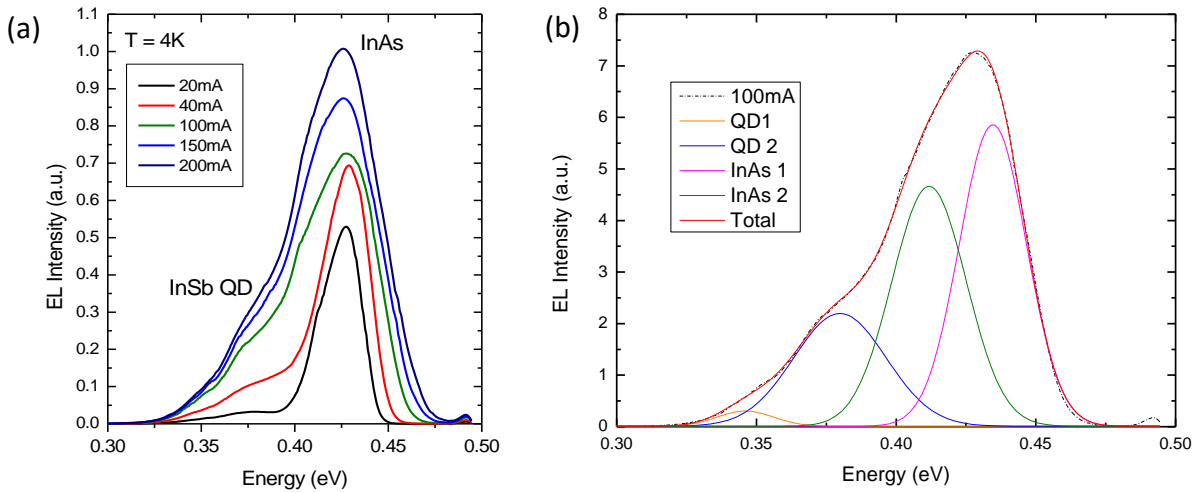


Figure 3: (a) EL Spectra at 4 K measured at various drive currents at 1 kHz and 50 % duty cycle. (b) Deconvolution of the spectra into 4 Gaussian functions corresponding to transitions from the InSb QDs (e-hh1-QD1 and e-hh2-QD2), and InAs.

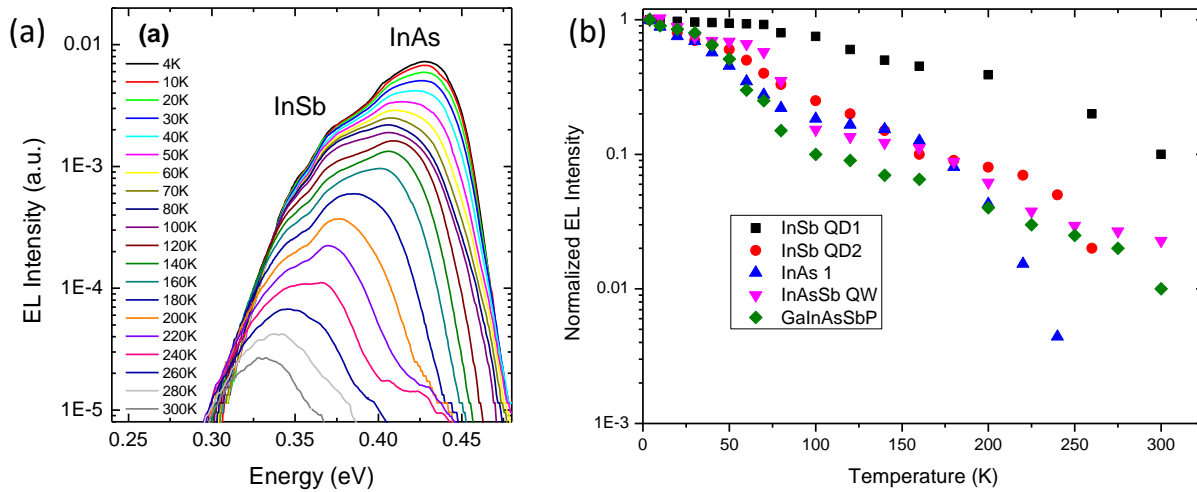


Figure 4: (a) Temperature-dependent EL spectra for the LED measured using an injection current of 100mA at 1 kHz, 50 % duty cycle. (b) Dependence of the integrated EL intensity for the InSb/InAs QD LED transitions along with reference InAsSb/InAs MQW and GaInAsSbP samples.

EL emission spectra from the LED measured at various temperatures using 100 mA quasi-cw excitation at 1 kHz are shown in figure 4a. Figure 4b plots the normalized intensity (normalized to 1 at 4 K) of the individual transitions from the InSb/InAs QD LED with temperature, along with LED reference samples operating at a similar wavelength reported previously (type II InAsSb/InAs QW⁸ and bulk GaInAsSbP LEDs⁹). Emission from the InAs quenches more rapidly and is suppressed at temperatures higher than 240 K due to Auger recombination which increases exponentially with temperature. The excited state QD emission quenches around 260 K due to the leakage of holes out of the QD whereas the ground state QD emission survives up to room temperature. The QD LED exhibits superior temperature quenching compared to the reference QW and bulk samples due to a lower level of Auger recombination as will be discussed below.

To eliminate the effects of Joule heating, the devices were tested at room temperature under pulsed conditions with a pulse width of 1 μ s and a frequency of 1 kHz (figure 5). A plot of Log L (Light Intensity) vs Log I (current) yields the gradient of $2/Z$ where Z takes the values of 1, 2 or 3 depending whether the dominant mechanism is Shockley Read Hall, radiative or Auger¹⁰. For the GaInAsSbP bulk LED, a value of $Z=3$ was obtained over the entire current range indicating that Auger recombination is the dominant mechanism. For the QW LED, $Z=2.4$ up to 200 mA but then switches to 2.8 indicating that Auger dominates at higher injection currents. For the QD LED, $Z=2.4$ over the entire current range suggesting mainly radiative recombination. We attribute the reduction of Auger recombination in the QDs due to the discrete density of states. Another possibility is that the reduction in Z could also be due to the increasing role of SRH recombination in the QD LED which is also consistent with the lower efficiency and the reduction in temperature quenching. Further studies using time-resolved PL measurements¹¹ are needed to fully clarify this which will be the subject of our future work.

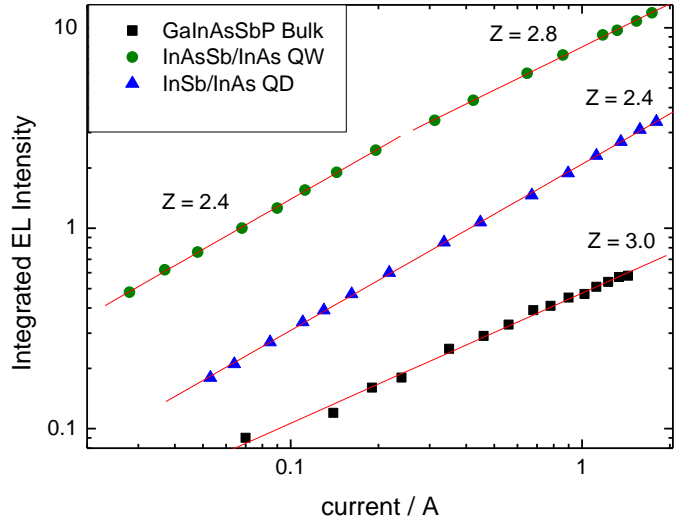


Figure 5: Integrated EL intensity from bulk GaInAsSbP, InAsSb MQW and InSb QD LEDs as a function of current on log scales measured at room temperature. The Z value is extracted from $2/\text{gradient}$ for each LED. The devices were tested using a pulse width of 1 μ s and a frequency of 1 kHz.

4. InSb QDs in InAs/AlAsSb ‘W’ quantum wells

One path to improve the performance of InSb/InAs QD structures is to increase the electron-hole (e-h) wavefunction overlap by confining the electrons. This will reduce the loss of electrons from the active region and reduce CHCC Auger recombination by reducing the number of states available for the electrons to scatter into. This can be done by inserting the InSb QDs in InAs QWs which are surrounded by AlAsSb layers in a ‘W’ arrangement¹² as shown schematically in figure 6. For 2.9 nm InAs wells the e-h wavefunction overlap is calculated to be around 75 %, much higher than 35-40% for conventional InSb/InAs QD structures discussed previously.

Structures were grown with a 0.4 μ m-thick AlAs_{0.92}Sb_{0.08} layer lattice-matched to GaSb, a 5 period ‘W’ QW active region and 10 nm-thick GaSb cap layer. Each period of the W QW active region includes AlAs_{0.08}Sb_{0.92} barriers of 23 nm thickness, 1-3 nm-thick strained ($\sim 0.6\%$ strain) InAs QWs with an InSb QD sheet in the centre. All the layers were grown at 430°C. Figure 7 shows the (004) X-ray diffraction (XRD) rocking curve from the sample containing 2.9 nm InAs wells where well defined satellite peaks can be observed. The low temperature PL spectra from samples containing InAs QWs of 18 and 29 Å widths are shown in figure 8. Peaks at 0.418 and 0.58 eV originate from the W QW-QD as a result of radiative recombination between electrons located in the InAs QW and holes localized in the InSb QDs. These results are encouraging and are the first step towards growth on mature GaSb substrates. Further improvements can be anticipated through optimization of the overall strain, which could be achieved through the use of tensile strained InGaAs barriers.

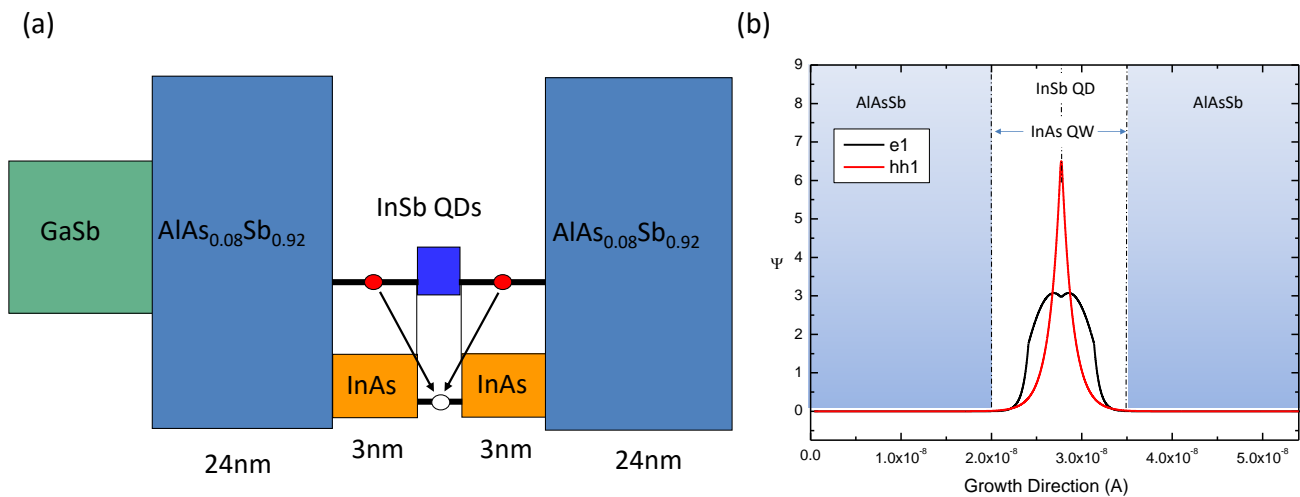


Figure 6: (a) Schematic bandstructure calculation of InSb/InAs/AlAsSb ‘W’ Structures and (b) e-h wavefunction overlap which is approximately 75 %.

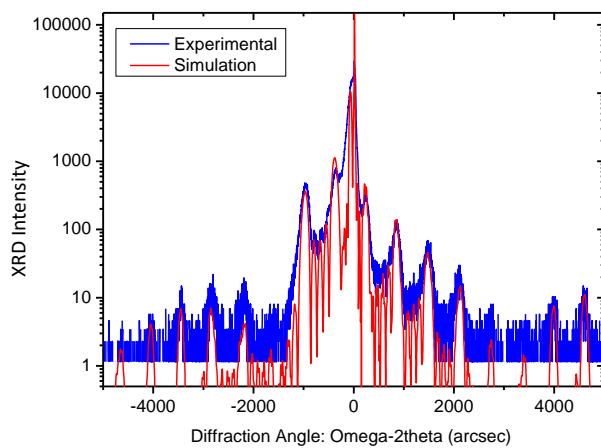


Figure 7: (a) High Resolution XRD spectra obtained from InSb/InAs/AlAsSb ‘W’ structures grown on GaSb with 2.9 nm InAs QWs.

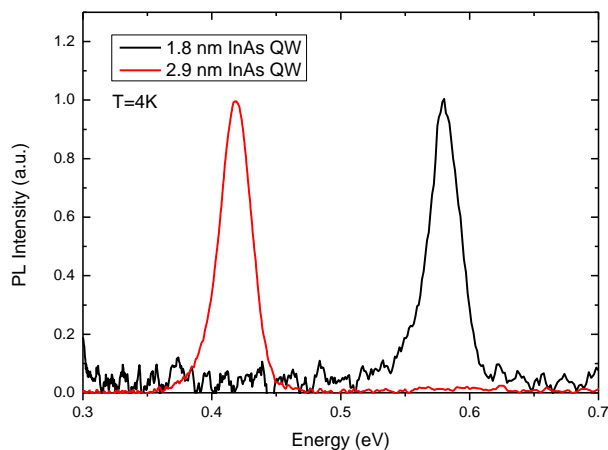


Figure 8: PL Spectra measured at 4K from the InSb/InAs/AlAsSb ‘W’ structures grown on GaSb which contain 2.9 nm and 1.8 nm InAs QWs.

5. Conclusions

In summary, the MBE growth and optical properties of InSb QDs have been studied. Dense arrays of InSb QDs were grown which are formed within InSb submonolayers in InAs. The QDs were grown with a novel technique that uses Sb-As exchange and MEE. LEDs were fabricated containing 10 InSb QD sheets and a 30 nm AlGaAsSb electron blocking barrier which showed bright EL peaking at 3.8 μm at room temperature. Analysis of the L-I curves showed that radiative recombination was the dominant mechanism at room temperature in the QD LED with superior temperature quenching and that Auger recombination had been suppressed. In comparison, QW and bulk LEDs were dominated by Auger recombination at room temperature. Finally multiple InAs/InSb/InAs/AlAsSb “W” QW-QD heterostructures were grown on GaSb substrates to increase the e-h wavefunction overlap. These samples demonstrated good structural quality and low-temperature PL around 3 μm .

6. Acknowledgements

Financial support for this work was provided from EPSRC (EP/N018605/1) and The EU Marie-Curie Training networks PROPHET (FP7 – 264687) and PROMIS (H2020-MSCA-ITN-2014-641899). P. J. Carrington and A. R. J. Marshall gratefully acknowledge support as fellowships from the Royal Academy of Engineering. We are grateful to Dr. Thomas Walther of Sheffield University for advanced microscopy and the STEM images.

References

1. Meriggi L, Steer MJ, Ding Y, Thayne IG, MacGregor C, Ironside CN, et al. Enhanced emission from mid-infrared AlInSb light-emitting diodes with p-type contact grid geometry. *Journal of Applied Physics*. 2015;117(6):063101.
2. Jung S, Suchalkin S, Kipshidze G, Westerfeld D, Golden E, Snyder D, et al. Dual wavelength GaSb based type I quantum well mid-infrared light emitting diodes. *Appl Phys Lett*. 2010;96(19).
3. Koerperick EJ, Norton DT, Olesberg JT, Olson BV, Prineas JP, Boggess TF. Cascaded Superlattice InAs/GaSb Light-Emitting Diodes for Operation in the Long-Wave Infrared. *Ieee J Quantum Elect*. 2011;47(1):50-4.
4. Tasco V, Deguffroy N, Baranov AN, Tournie E, Satpati B, Trampert A, et al. High-density InSb-based quantum dots emitting in the mid-infrared. *J Cryst Growth*. 2007;301:713-7.
5. Carrington PJ, Solov'ev VA, Zhuang Q, Krier A, Ivanov SV. Room temperature midinfrared electroluminescence from InSb/InAs quantum dot light emitting diodes. *Appl Phys Lett*. 2008;93(9).
6. Lu Q, Zhuang Q, Hayton J, Yin M, Krier A. Gain and tuning characteristics of mid-infrared InSb quantum dot diode lasers. *Appl Phys Lett*. 2014;105(3).
7. Solov'ev VA, Lyublinskaya OG, Semenov AN, Meltser BY, Solnyshkov DD, Terent'ev YV, et al. Room-temperature 3.9-4.3 μm photoluminescence from InSb submonolayers grown by molecular beam epitaxy in an InAs matrix. *Appl Phys Lett*. 2005;86(1).
8. Krier A, Smirnov VM, Batty PJ, Vasil'ev VI, Gaggis GS, Kuchinskii VI. Room temperature midinfrared electroluminescence from GaInAsSbP light emitting diodes. *Appl Phys Lett*. 2007;90(21).
9. Carrington PJ, Zhuang Q, Yin M, Krier A. Temperature dependence of mid-infrared electroluminescence in type II InAsSb/InAs multi-quantum well light-emitting diodes. *Semicond Sci Tech*. 2009;24(7).
10. Mirza BI, Nash GR, Smith SJ, Buckle L, Coomber SD, Emeny MT, et al. Recombination processes in midinfrared Al(x)In(1-x)Sb light-emitting diodes. *Journal of Applied Physics*. 2008;104(6).
11. Høglund L, Ting DZY, Soibel A, Hill CJ, Fisher AM, Keo SA, et al. Minority Carrier Lifetimes in InSb/InAsSb Quantum Dot and InAsSb nBn Photodetectors. *Ieee Photonic Tech L*. 2015;27(23):2492-5.
12. Meyer JR, Hoffman CA, Bartoli FJ, Rammohan LR. Type-II Quantum-Well Lasers for the Midwavelength Infrared. *Appl Phys Lett*. 1995;67(6):757-9.